Singapore-ETH Centre; Wuhan University; Artescan, Portugal

JOINT PROCESSING OF UAV IMAGERY AND TERRESTRIAL MMS DATA FOR VERY HIGH RESOLUTION 3D CITY MODELING

Armin Gruen, Xianfeng Huang, Rongjun Qin, Tangwu Du, Wei Fang, Joao Boavida, Adriano Oliveira

Abstract: Both Unmanned Aerial Vehicles (UAV) technology and Mobile Mapping Systems (MMS) are important techniques for surveying and mapping. In recent years, the UAV technology has seen tremendous interest, both in the mapping community and in many other fields of application. Carrying off-the-shelf digital cameras, the UAV can collect high resolution aerial images for city modeling using photogrammetric techniques. In addition, a MMS can acquire high density point clouds of ground objects along the roads. The UAV, if operated in an aerial mode, has difficulties in acquiring information of ground objects under the trees and along façades of buildings. On the contrary, the MMS collects accurate point clouds of objects from the ground, together with stereo images, but it suffers from system errors due to loss of GPS signals, and also lacks the information of the roofs. Therefore, both technologies are complementary.

This paper focuses on the integration of UAV images, MMS point cloud data and terrestrial images to build very high resolution 3D city models. The work we will show is a practical modeling project of the National University of Singapore (NUS) campus, which includes buildings, some of them very high, roads and other man-made objects, dense tropical vegetation and DTM. This is an intermediate report. We present work in progress.

Keywords: Unmanned Aerial Vehicles (UAV), Mobile Mapping Systems (MMS), data integration, city modeling

GEMEINSAME VERARBEITUNG VON UAV-BILDERN UND TERRESTRISCHEN MMS-DATEN ZUR GENERIERUNG HOCHAUFLÖSENDER 3D-STADTMODELLE

Zusammenfassung: Unmanned Aerial Vehicles (UAV) und Mobile Mapping Systeme (MMS) sind wichtige Technologien in der Geomatik. In den letzten Jahren hat die UAV-Technologie in der Geomatik sowie in anderen Anwendungsbereichen einen beispiellosen Aufschwung erlebt. Unter Benutzung handelsüblicher digitaler Kameras können hochauflösende Luftbilder erzeugt und diese mithilfe photogrammetrischer Methoden zur Erstellung von 3D-Stadtmodellen verwendet werden. Zusätzlich kann ein MMS hochauflösende Punktwolken von Objekten entlang von Straßen generieren. Falls das UAV im Luftbildmodus betrieben wird, hat es Probleme, Objekte unter Bäumen und an Fassaden von Gebäuden aufzunehmen. Andererseits sammelt das MMS gerade Informationen von Objekten aus einer terrestrischen Perspektive, möglicherweise sogar zusammen mit Stereobildern. Jedoch gibt es im Stadtbereich große Probleme mit dem Verlust des GPS-Signals, und es fehlen auch Informationen über die Dächer. Daher müssen beide Technologien als komplementär betrachtet werden.

Dieser Beitrag behandelt die Integration von UAV-Bildern, MMS-Punktwolken und terrestrischen Bildern zum Zwecke der Generierung von sehr hochauflösenden Stadtmodellen. Wir beschreiben die Arbeiten zur Erstellung eines 3D-Modells des National University of Singapore (NUS) Campus, bestehend aus Gebäuden (einige davon extrem hoch), Straßen und anderen von Menschen errichteten Objekten, dichte tropische Vegetation und ein DTM. Dies ist ein Zwischenbericht. Wir präsentieren die Ergebnisse laufender Arbeiten.

Schlüsselwörter: Unbemannte Luftfahrzeuge (UAV), Mobile Mapping Systeme (MMS), Datenintegration, Stadtmodellierung

Authors

Prof. em. Dr.-Ing. Armin Gruen
Rongjun Qin, M. Sc.
Tangwu Du, M. Sc.
Wei Fang, M. Sc.
Singapore-ETH Centre
Future Cities Laboratory
1 CREATE Way
#06-01 CREATE Tower
Singapore 138602
Singapore
E: agruen@geod.baug.ethz.ch
   rqin@student.ethz.ch
   tangwudu@gmail.com
   wei@arch.ethz.ch

Dr. Xianfeng Huang
LIESMARS
Wuhan University
No. 129, Luoyu Road
Wuhan 430079
PR China
E: hwangxf@gmail.com

Eng. Joao Boavida
Eng. Adriano Oliveira
Artescan – 3D Scanning Lda
IPN Incubadora, Rua Pedro Nunes
3030-199 Coimbra
Portugal
E: jboavida@artescan.net
   adrianooliveira@artescan.net

1 INTRODUCTION

Today 3D city models are important base datasets for many applications, some more traditional, other quite new. The efficient generation of high resolution structured models (not just unstructured surface models) is both a relevant research topic and an important issue for the professional practice. Both Unmanned Aerial Vehicles (UAV) and Mobile Laser Scanners (MLS) are important techniques for surveying and mapping. UAV technology, if used in aerial mode, and terrestrial Mobile Mapping Systems (MMS) are complementary technologies. While aerial UAV images are ideally suited to model the roof landscape and part of the terrain, terrestrial point clouds are able to look under the trees and also to represent the façades. If these two datasets are amended by terrestrial images we have most of the primary information needed to generate a complete 3D city model.

Integration of multiple sensor data can add more information and reduce uncertainties in data processing, also allow for a higher degree of automation. Most of the multi-source data fusion research is built on data from similar view directions, like the airborne LiDAR point clouds and images from aerial and satellite platforms. For city modeling the integration of data through the use of complementary data sources can be helpful for both building detection and model reconstruction. However, only few researchers have worked on integrating data from airborne and ground based sensors. Von Hansen et al. (2008) proposed a method using extracted straight lines to register airborne and terrestrial laser scanning data. Stewart et al. (2009) combined and positioned the terrestrial laser scanning data to airborne LiDAR data to detect ground displacements caused by natural hazards. Rutzinger et al. (2009) proposed a method to extract vertical walls from terrestrial mobile and airborne laser scanning data. Al-Manasir & Fraser (2006) georeferenced terrestrial laser-scan data with the
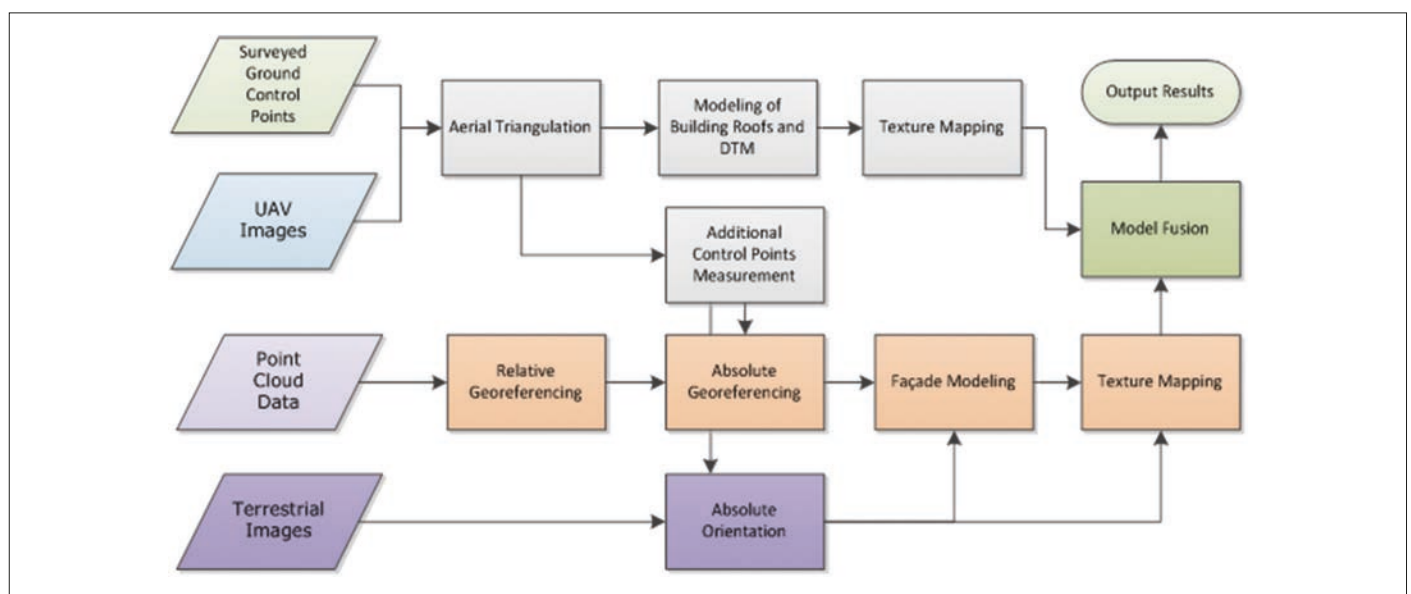

Figure 1: Flowchart of the data processing steps

help of terrestrial images via signalized common points.

On the other hand, most of the past UAV applications are performed in rural or suburban areas, such as cultural heritage site modeling, suburban mapping, agriculture monitoring, etc. (Eisenbeiss 2009, Gruen et al. 2012). Only few projects are reported about mapping urban areas with UAV, and even more seldom is the combination of UAV images with MMS point clouds for city modeling. How to combine and how to use them are the key issues in this paper.

This paper focuses on the integration of UAV images and MMS point clouds to build a very high-resolution 3D city model. This work will show a practical modeling project of the Campus of the National University of Singapore (NUS), which includes DTM, buildings and other man-made objects, and dense tropical vegetation. Our contribution will be:

(a) Very high resolution roof landscape models from UAV image data,
(b) Accuracy evaluation of the georeferencing of point clouds by using UAV image data,
(c) Modeling buildings with their façades from laser point clouds and terrestrial images,
(d) Setting an example of integration of these three data sources for 3D city modeling,

which, according to our knowledge, has not been done before. Fusion is done both on the level of data processing and data integration.

2 MAIN PROCESS WORKFLOW

The input of our work is: (1) Raw point clouds from MMS; (2) UAV images; (3) Few Ground Control Points (GCP); (4) Terrestrial images for geometric modeling and (5) optional: Texture mapping from aerial

Figure 2: The NUS modeling area. Different colors show different areas separated by roads (courtesy: Google Earth).

and terrestrial images. Our working procedure can be summarized into several steps, including:

(a) UAV images aerial triangulation;
(b) Integration of UAV-derived control point data to georeference and adjust the MMS point cloud data;
(c) Modeling of the roof landscape from UAV images;
(d) Measurement of the DTM from UAV images;
(e) 3D modeling of façades from MMS data and (if needed) from terrestrial images;
(f) Modeling of DTM from MMS and topo map data;
(g) Fusing façade and roof models and the DTMs to generate a complete geometry model;
(h) Optional: Texture mapping from aerial and terrestrial images.

The complete procedure is shown in Figure 1. From the input image data, control points and raw point cloud data, we can achieve a complete 3D site model,

achieved by integration of these input data sources. One of our byproduct is a accurately georeferenced point cloud data, derived from existing aerial image data without extra surveying field work.

## 3 UAV IMAGE DATA COLLECTION AND PROCESSING

3.1 UAV IMAGE DATA ACQUISITION

The modeling area covers the main campus of the National University of Singapore of approximately 2.2 km². This may not be a large area in mapping, but considering the flying height of 150 meters and a camera constant of 16 mm with an off-the-shelf camera, we obtained 929 images in total. An additional problem was generated by the fact that the terrain has 70 m height differences and the highest building is about 100 m high – compared to the flying height an object with a tremendous three-dimensionality.

The aerial image collection has been done by the AscTec Falcon 8 octocopter system, developed by Ascending Technologies GmbH, with an off-the-shelf camera Sony Nex-5. It is a two-beam octocopter with four rotors on each side, powered by battery. It has a build-in GPS/IMU, a barometer, electronic compass and a stabilizing system for both the camera and the platform. It has up to 300 meters remote controlling distance with a maximal operation slot of 20 minutes. Limited by this short flying time of the platform, the image data collection had to be done with 43 starts and landings in three days, because each flight collected only a small block of 4 x 4 or 5 x 5 images. After data cleaning, we finally used 857 images out of the total of 929 images with corresponding GPS/IMU records. The layout of the block is shown in Figure 4 (left). In order to minimize occlusions we designed the block with 80%

Figure 3: Examples of take-off and landing in confined urban areas
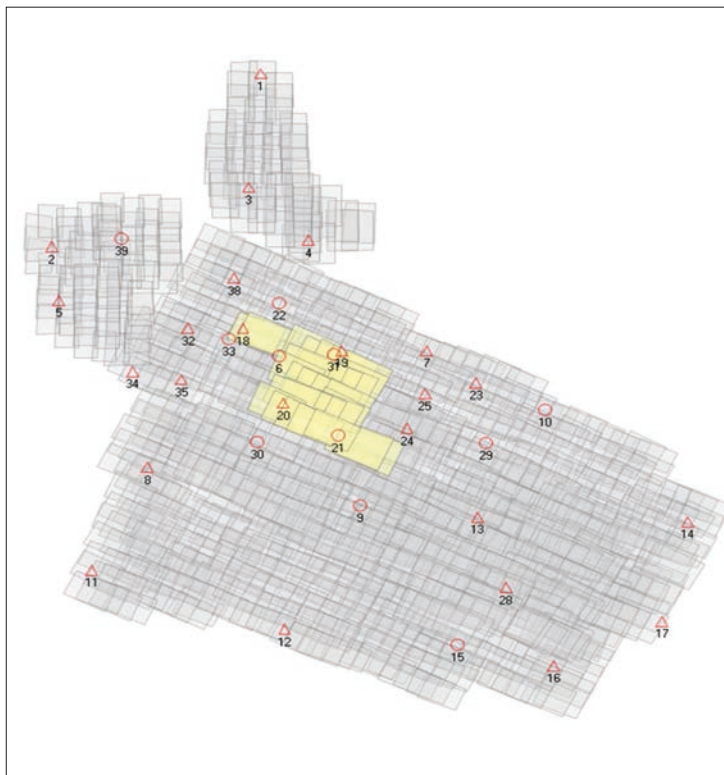
Figure 4: *Layout of the NUS image block (left) and a sample image of high-rise buildings (right). Triangles: Control points. Circles: Check points. Area highlighted in yellow: Sub-block for geo-referencing test.*

in-strip and 60% across-strip overlap. The right part of Figure 4 shows a sample image with 5 cm ground resolution.

There was another restriction concerning the flight: the octocopter was not allowed to fly across the major public roads and should stay strictly within the campus boundaries, which splits the whole area into three parts (Figure 2). This required the flight path to follow the border of the campus closely.

Comparing to a fixed-wing platform, a helicopter-type platform has several advantages, which make it particularly useful in a densely built-up urban environment:

1. It does not need a runway or ejection devices.
2. The take-off and landing space can be relatively small and confined.
3. The mission can be terminated directly when unexpected situations happen, such as strong wind, unexpected rain or the approaching of another flying object.
4. Image acquisition can be done in a discrete mode by hovering when taking images, which can reduce the motion blur during the operation.
5. It can collect images in a vertical flying mode. This may be of interest in particular applications, e. g. when data for façade modeling is collected.

During the practical operation take-off and landing are the most demanding issues. The ideal situation for take-off and landing is on the roofs of houses, if relatively large and open spaces are available (minimum 5 x 5 m² is suggested). However, most of the roofs are not accessible. Since Singapore is a typical tropical country, and there are a lot of complex cooling systems on the roofs, the spaces on roofs are usually quite confined. In this case, the take-off and landing spaces are mostly restricted to the ground: pedestrian ways, playgrounds, parking lots, etc. (Figure 4). During the take-off and landing, the biggest challenge is to avoid large tropical plant canopies and man-made structures. Therefore we used the manual mode for take-off and landing for a more flexible performance, and then switched to automatic waypoint mode after the octocopter rose to a certain height.

Due to the complex infrastructures with different functionalities in urban areas, which may create electro-magnetic disturbances, the loss of signal happened quite often. In this case, the pilot needs to move around for an appropriate angle and distance to get the signal back. Therefore, it is suggested to perform the operation early in the morning, when less human activity and radio disturbances are involved. Our data

acquisition took three days of field work, which, for safety reasons, could only be done during weekends.

Ideally, the produced images and GPS/IMU records should match perfectly, but our actual data contained a fair amount of deviations, which can be divided into two types: (1) The GPS/IMU values do not match the images. (2) More images are taken automatically beyond the planned numbers. Those problems may come from the electro-magnetic disturbances which misguide the remotely controlled signals, or bugs in the system software. Therefore, data cleaning took quite some time. We wrote some scripts to accelerate the process by checking image overlaps, deleting images with too much overlap, getting rid of repeatedly taken images, and detecting GPS points which deviated too much from the mean position of the block.

The Sony Nex-5 is a mirror-less interchangeable lens camera, with an image dimension of 4.592 x 3.056 and a pixel size of 5 μm in both x and y directions. We used a lens with a fixed focal length of 16 mm. This camera is well commented in photography, but as we found, the lens has a fair amount of color refraction, leading to blurring problems in the image corners.

The camera calibration was done in our lab with the software package IWit-

Figure 5: Left: Mobile Mapping System. Middle: Example point cloud data at CREATE buildings. Right: MMS NUS campus trajectory.

ness, using the point cloud calibration method (Remondino & Fraser 2006). The calibration resulted in a standard error of image coordinates of 0.24 pixels.

3.2 UAV IMAGE AERIAL TRIANGULATION WITH DIFFERENT SOFTWARE PACKAGES

Our geo-referencing process was divided into two stages:

1. Test the triangulation and bundle adjustment with a small subset of all images of this mission. We took the images from one flight as a small subset. To include more GCP for the test we added four more images in the block corners (Figure 4 left, highlighted in yellow).

2. Try to do the geo-referencing of the full block with different software packages according to their performance in the small block. The small block tests were performed because it is easier to analyze data in a small dataset. We assumed that if a software package will fail with the small block it will inevitably also fail with the full block. For the full block, we acquired 39 control points with Trimble GPS, with an accuracy of 2 cm in x, y direction, and 3 cm in height. The distribution of the GCP is shown in Figure 4. In the small block triangulation, points 18, 19, 20, 21 are used as GCP and the others are used as check points.

We also used the small block for an accuracy analysis of the measured exterior orientation parameters. For this purpose we compared the GPS/IMU measured values with the results from bundle adjustment, which were considered the correct values. The positional values, as determined by GPS, have maximal values at 4.7, 9.1,

3.2 m for X, Y, Z. But they include a large bias (shift), which, if removed, gives coordinate accuracies for X, Y, Z of about 1 m. The attitude values have maximal deviations of 12.9, 9.2, 3.1 deg for roll, pitch, yaw, and the removal of a shift bias will improve the standard deviations to 3.8, 5.6, 0.8 deg.

The control point distribution for the full block is not ideal, because, due to occlusions by tropical vegetation and other objects, the optimal locations could not be realized. We performed the geo-referencing of the small block with several pieces of commercial and non-commercial software. Most of the software tested in our mission worked relatively well and we obtained an accuracy of about 5 cm in horizontal, and 5-8 cm in vertical direction. However, when it comes to the full block processing we were running into problems with geo-referencing, which will be addressed in the following.

Leica Photogrammetry Suite (LPS)

LPS is a popular commercial software package for geo-referencing due to its easy-to-use interface and compatibility with a variety of sensors. This software is not specifically designed for UAV imagery. LPS has two modes of tie point measurement: (a) Given an estimation of the exterior orientation parameters, LPS will look for corresponding points along the computed epipolar line by correlation methods. (b) After measurement of three or more points per stereo-pair manually as seeds, LPS will generate additional tie points automatically.

The first mode depends on the quality of initial exterior orientation parameters. We imported the recorded GPS/IMU data as

the initial exterior orientation parameters, but it failed because of the poor quality of this data. The second mode could be a valid way when the dataset is small, but it is not reasonable to manually measure the tie points on 857 images. Therefore, we wrote a separate program to generate tie points with the Sift operator (Lowe 2004): It first generates Sift features and looks for neighboring images of each image by the recorded GPS position. Image matching is applied with Sift features in the neighboring images. Finally a Ransac algorithm (Zuliani et al. 2005) based relative orientation is performed to orient all the images for detecting blunders and a LPS-formatted tie point file is output. After the tie points stage, we measured the controls points manually and run the bundle adjustment. We used self-calibration by releasing focal length, principal point and radial distortion. This works well with the small test data set, but it fails for the full set. We received RMSEs for planimetry at 0.13 m and 1.6 m for height. Given a pixel size of 5 cm this is not acceptable. Since the LPS software is largely a black box for the user we could not give an explanation for the failure.

APS (Aerial Photo Survey) from Menci Software

APS is a fully automatic software package in which a fairly small amount of interaction is involved. It is originally designed for images acquired by the Swinglet from sense-Fly, while it can also handle images from other UAV platforms. The software requires as input lat/lon/height/heading/pitch/roll, and if a different exterior orientation system is used, the user needs to convert the values externally. However, due to the high automatic workflow, the software pro-

vides limited customized settings to adjust the performance of the bundle adjustment. In our case it has a fair performance in bundle adjustment in an arbitrary coordinate system, but it does not perform well when GCP are involved. It leads to a maximal residual of more than 0.5 meters for check points within the small test block. Therefore we only did bundle adjustment of the whole dataset in an arbitrary coordinate system, and finally it succeeded to orient all the images with a re-projection error of about 2 pixels.

MATCH-AT and a customized tool from Graz University

INPHO helped us to test the Match-AT module with our dataset. It failed to get the required accuracy. A customized software package from Graz University, which implicitly uses the method proposed in (Irschara et al. 2010, Maurer et al. 2012) was also tested with the dataset. It can robustly orient the dataset and kick out images which have large re-projection errors. It finally oriented 600 images, with a re-projection error of 1-2 pixels. In its version of the time of computation the software was not able to incorporate the GCP into the bundle adjustment.

pix4d

pix4d is fully automatic, easy to operate and supports different coordinate systems

and datums. Manual tie point measurement is supported in monoscopic mode. It delivers a good report for the bundle network adjustment in terms of the connectivity between images, and GCP residuals in both object space and image space.
Disadvantages:
▶ The parameter settings for the bundle adjustment are hidden, GPS/IMU values are not used as observations but only in the pairwise image matching process (X,Y is needed only). The only accessible parameters are GCP weights and whether to use self-calibration or not.
▶ There is no covariance matrix for the orientation parameters and the self-calibration parameters.
Our data set was processed with pix4D but we did not use the results at that time because the black box character of the software left some uncertainties.

APERO

APERO is an open source tool developed by the French National Geographic Institute (IGN) (Deseilligny & Clery 2011). Given the rough position from GPS of each image, the software can find the relationships between images. Then the tie points are extracted automatically by the SIFT algorithm and a following exhaustive search strategy deals with failure in matching. The RMSEs computed from 11 check points

give 7 cm planimetric and 6.5 cm height accuracy. These values, slightly above the one-pixel mark (5 cm) are acceptable considering the fact that we are dealing here with natural control and check points.

4 POINT CLOUD DATA COLLECTION BY MMS AND PROCESSING

The MMS (Mobile Mapping System) from ARTESCAN uses a RIEGL WMX-250 system, which consists of two RIEGL VQ-250 laser scanners, an IMU/GPS unit, a distance measurement indicator, and two calibrated optical cameras. The system can collect time stamped images and dense point clouds with a measurement rate up to 600 kHz and 200 scan lines per second. Figure 5 shows the system installed on a car (left) and a sample of the point cloud data of the CREATE area (middle), located inside NUS campus, rendered according to the intensity value.

Altogether, 34.4 GB of raw point cloud data of 16 km road sides were collected within 3 hours, with 5.25 GB sequences of stereo street images. The point cloud data is stored separately in 54 files. Figure 5 (right) shows the overview of the colored point cloud data with 700 points/m^2 in the middle part of the road. The left part of Figure 6 shows the interpolated intensity data along the trajectory. We interpolated the intensity data with 2.5 cm sample space and normalized the intensity values
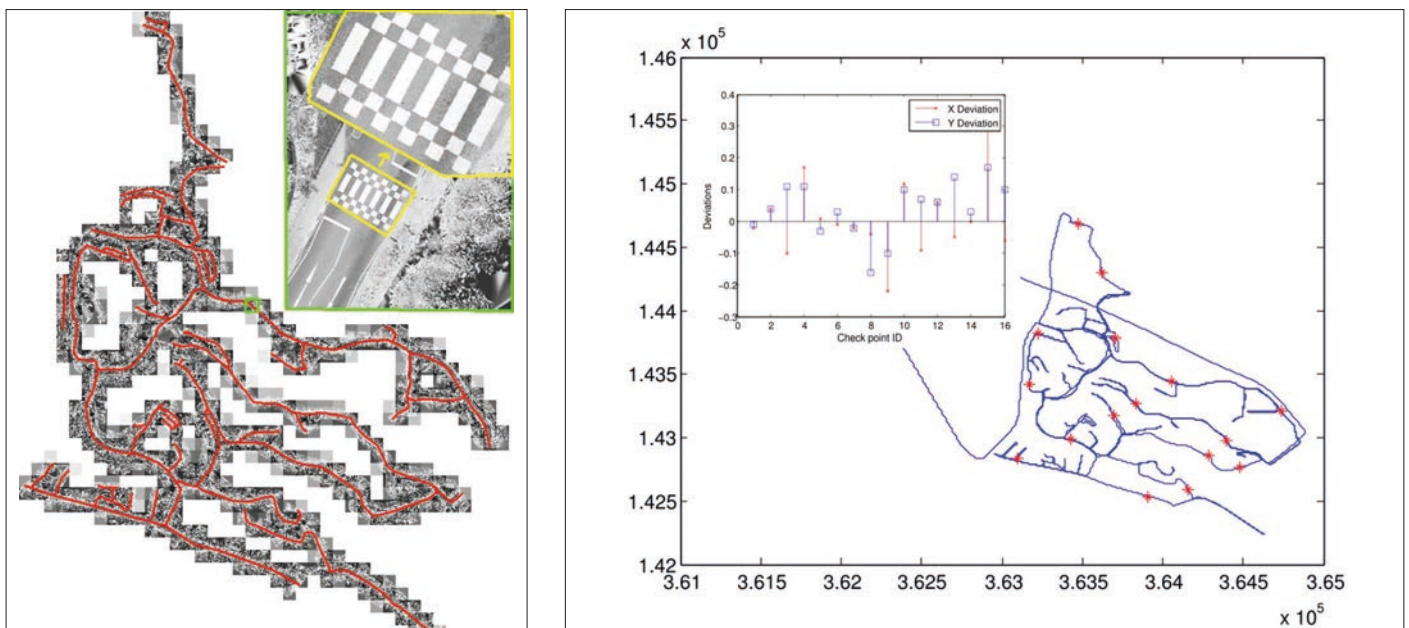
Figure 6: Left: Overview of NUS campus point cloud intensity data. Right: Distribution of check points and their coordinate differences at X and Y directions (unit: meter).

Figure 7: Results of NUS campus modeling. Left: UAV image with non-relevant roof sub-structures. Middle: UAV image. Right: Zoom-in result of the textured building model.

to grey level for visualization, as shown in the upper part of the left image in Figure 6. The intensity data of the point clouds has very stable quality along the road, showing clear corners and edges of road marks, such that it provides great potential for us to measure corresponding points between images and point clouds precisely.

Point Cloud Data Adjustment

As there are many high buildings and dense trees which partially block the GPS signals, the coordinate accuracy of GPS is not very high, thus influencing negatively the accuracy of the trajectory after fusion of GPS and IMU. The GPS signal losses happen frequently and unpredictably, so it needs many control points to re-georeference the point clouds.

These control points were measured from georeferenced stereo UAV images. Altogether, 169 control points have been measured manually from the stereo UAV images. To verify the accuracy of manual measurements, a group of points were measured four times and the differences of coordinate values between the four measurements were evaluated. As a result, the average measurement errors in X, Y and Z directions are 2.8 cm, 3.7 cm and 4.8 cm. Compared to the accuracy of the point cloud data before adjustment, these errors are relatively small, such that we can use the points for georeferencing of our mobile mapping point cloud data.

The software used for trajectory adjustments was RIEGL's RiProcess, designed for managing, processing, and analyzing data acquired with airborne and terrestrial mobile laser scanning systems. A two-step procedure was applied to adjust the data using control points from point clouds. The locations of these control points were chosen regarding criteria like spatial distribution, but also at crossroads where there are
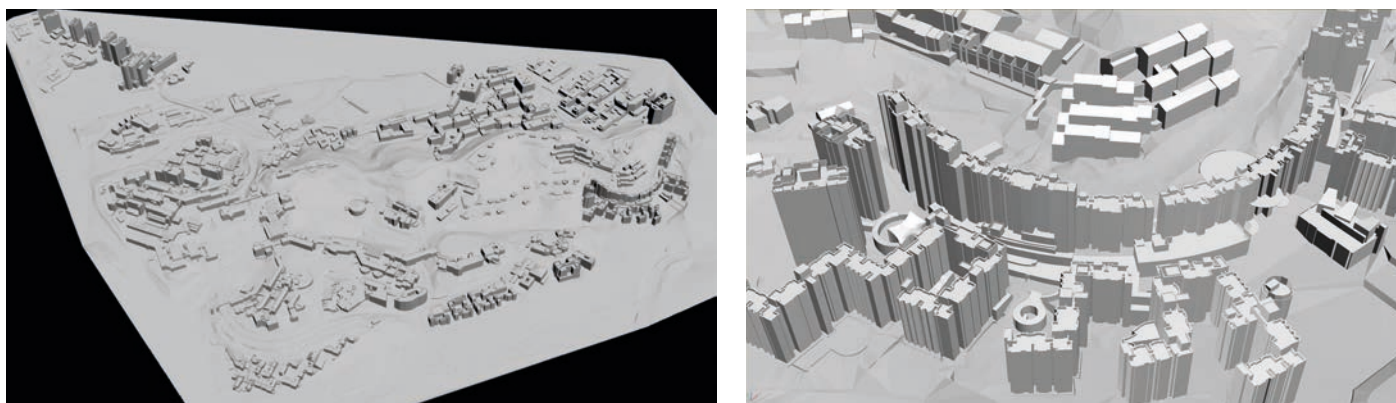
Figure 8: DTM and building models of the NUS campus. Left: Overview. Right: Section zoom-in.
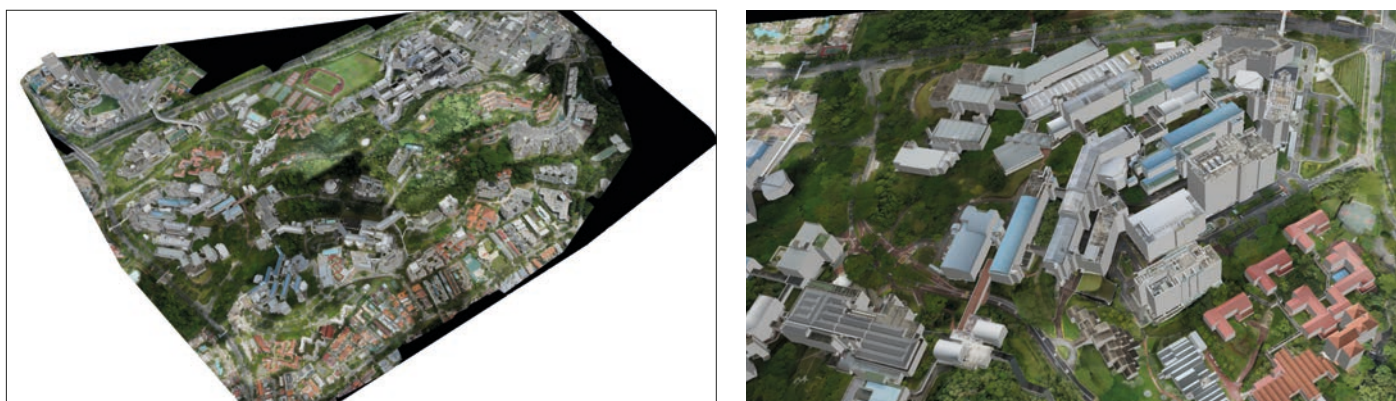
Figure 9: Textured model of NUS campus. Left: Overview. Right: Engineering section zoom-in.

(a)   (b)   (c)   (d)
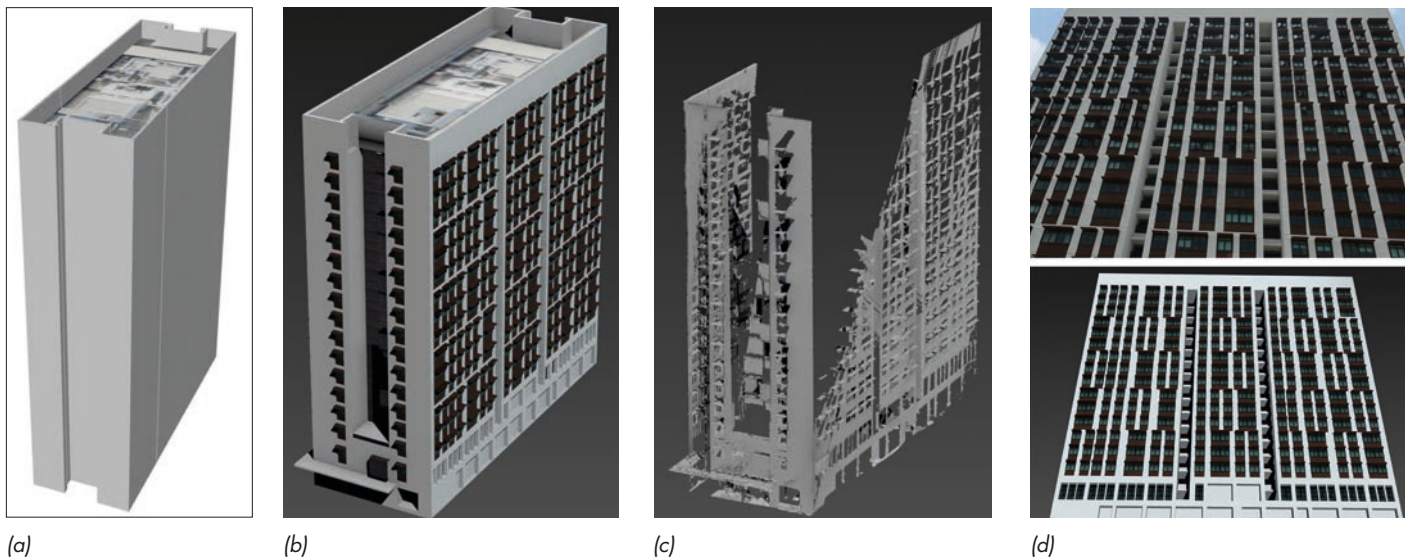
Figure 10: Example of a complete building model. (a) Roof model from UAV images. (b) Wrapped mesh from MMS point clouds. (c) Complete model by integrating roofs and façades. (d) Façade image (up) and 3D model (down).

overlapping areas from different passages. In these overlapping areas the adjustment was done in two steps, first relative, then absolute to the control points. After the trajectory was adjusted by given control points, the new trajectory was applied to re-calculate the coordinates of point clouds.

Accuracy Evaluation

The data accuracy check was conducted on newly measured check points, rather than on the control points used in the adjustment. We manually measured 16 points from both UAV stereo images and point cloud data. The check points are evenly distributed over the whole area along the roads, as shown in Figure 6. They were measured carefully at the corner of land marks or at places where we could easily identify the corresponding position.

Both data sets are based on the UTM projection system. But the height values of the UAV image data is based on WGS84 ellipsoid heights, while the point cloud data carries orthometric heights. As the test area is quite small (only 2.2 km²) and there is no big mountain causing gravity anomalies in such a small area, we can assume that the height differences between orthometric and ellipsoidal heights can be replaced by a constant value.

After the refinement of the georeferencing of the point cloud data, the inaccuracy of data due to GPS signal losses will be greatly reduced. Before georeferencing the point clouds to the control points

there was an average deviation of 0.4 m in planimetry and 0.6 m in height, with a maximal height deviation of 1.3 m. The inset in Figure 6 (right) shows the graph of residual distribution at X and Y directions after adjustment. An accuracy analysis of the georeferencing resulted for the 16 check points in the RMSE values of 11 cm for planimetry and 20 cm for height. These are values which could be expected given the cumulative error budget of UAV images and laser-scan point clouds.

5 3D MODELING COMBINING POINT CLOUD AND IMAGE DATA

5.1 BUILDING MODEL RECONSTRUCTION USING UAV IMAGE DATA

The building models have been created using the semi-automatic modeling software CyberCity Modeler (Gruen & Wang 1998). Giving weakly ordered key points of roofs measured on a Digital Workstation, following a set of criteria, it will automatically generate roof faces and wall faces, where only a small amount of post-editing is needed. It greatly reduces the operation time for constructing building models and can generate thousands of buildings with a fairly small work force. It is invariant to model resolution, and is also able to generate fine details on building roofs such as air-condition boxes, water tanks, etc. We used ERDAS StereoAnalyst as Digital Workstation and implemented a converter between StereoAnalyst and CyberCity Modeler.

A major problem is to decide what needs to be modeled and what not. This issue becomes the more pressing the finer the image resolution is (compare structure on the roof of the building in Figure 7 left). We decided to only model permanent architectural features and not facilities for air-condition and similar infrastructures, which may have temporal character.

A part of the building modeling result is shown in Figure 7. Figure 8 shows all buildings and the DTM, Figure 9 the textured model and a zoom-in of the Engineering section.

5.2 TERRAIN MODELING

We did some initial tests with automated image matchers for producing a DSM. The results, as expected, were by far not good enough. We will report about these tests elsewhere.

The DTM was generated from four data sources:

(a) Measurements from UAV images;
(b) Ground points from MMS point clouds;
(c) Tacheometric measurements for a high-precision hydrological test field;
(d) Digitized contours from an older topographic map 1:5,000.

The need to apply such multi-source approach was caused by the fact that a complete DTM could only be generated by combining these diverse sources. Large areas were covered by tropical trees, such obstructing the aerial UAV views onto the terrain. The MMS car could only drive on
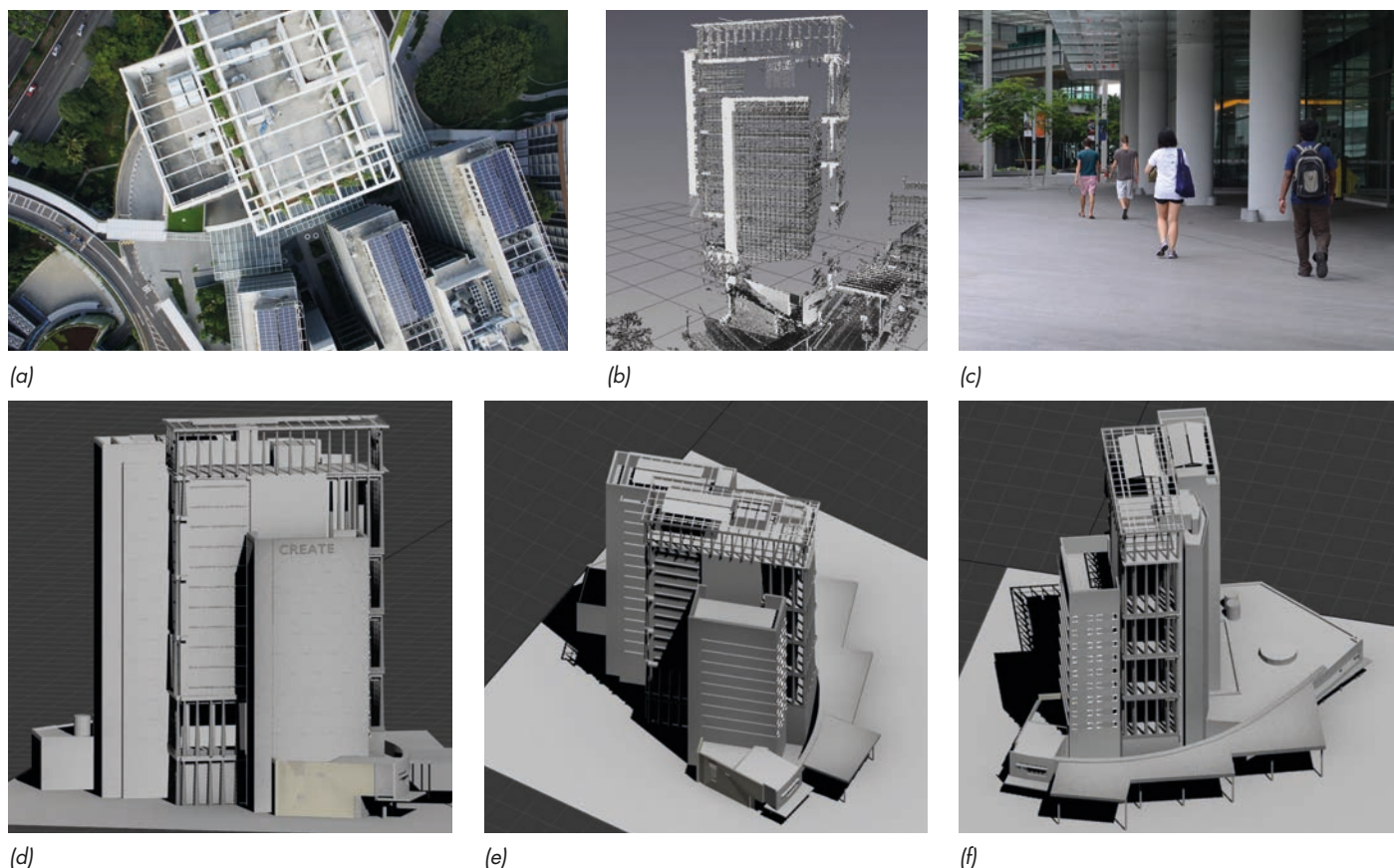
Figure 11: Model of the complex CREATE building. (a) Image from the UAV. (b) Sample point cloud from the Mobile Mapping system. (c) Terrestrial image sample collected by NIKON D7000. (d) (e) (f) Views onto the 3D model of the CREATE building, produced by integrating the data from UAV, point cloud and terrestrial images.

roads and as such missed large areas. The tacheometric measurements and the digitized contour lines gave us height information which otherwise was not accessible.

The result of data integration can be seen in Figure 8, it shows a combination of DTM and building models.

5.3 FAÇADE MODELING

After georeferencing of the point clouds using control points from UAV data, the two datasets could be registered together. The roof models from the stereo UAV images could serve as building contour, which is a compensation for the incompleteness of the MMS point cloud, thus making it easier to model the façade from occluded point clouds. The façade modeling in this project was done manually in 3ds Max. To make the modeling procedure easier, the point clouds was wrapped into a surface mesh model and imported into 3ds Max as reference. The roof model from the photogrammetric measurements of the same building was also imported into 3ds Max. Ideally, both model parts should match. In reality, the boundaries of the façades from point clouds show a small deviation to the boundary of roofs from UAV images. This had to be adjusted. For parts of the façade without point clouds, the complete façade structure could be deduced from the regular pattern of windows and
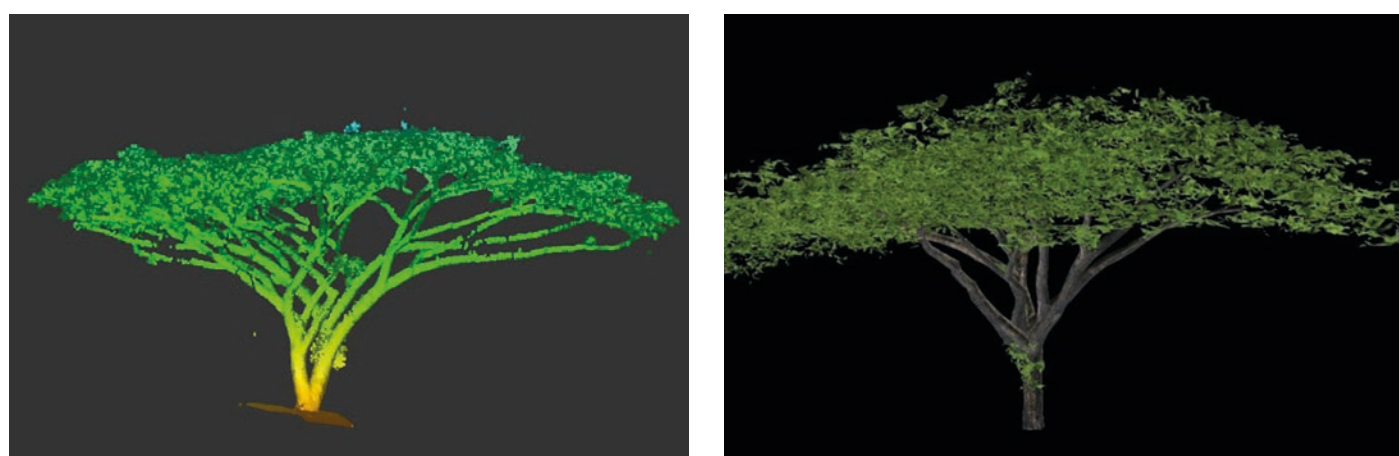
Figure 12: Rain tree modeled from the MMS point cloud. Left: Colored point cloud. Right: Tree model.

other façade features. Moreover, terrestrial or oblique images of façades could also provide further information for this modeling. Figure 10 shows an example of the generative process for a building model with roof structures and façades.

We also took terrestrial stereo images of an area called "University Town" for 3D façade modeling. Figure 11 shows the sample data and the modeling results of the most complicated building in University Town, the CREATE building. This building has a big volume and very complex structures, including solar panels on the roof, bars on the façades to stop the hot wind going up, etc. Actually, the building is so large that one image cannot cover the whole building. We had to measure each part of the roof and then combine the roof parts into a complete model. The façades were modeled using 3ds Max from wrapped point clouds. For the detailed structures which cannot be seen from UAV images or Mobile Mapping point clouds we took

terrestrial pictures using a NIKON D7000 camera. With the help from these images, we could model the inside structures. As shown in Figure 10, the detailed structures could be created with the help of integrated multiple data sources.

5.4 MODELING OF TREES AND LAMP POLES

Having strong tropical vegetation, dense trees and bushes are significant objects at NUS campus which post a challenge for modeling. We applied two different techniques for tree measurement and modeling. From the MMS point cloud we could derive very detailed and realistic tree models, which requires a lot of manual work. The corresponding steps and the used software are:

(1) Pointools Edit. Separate point cloud of a tree from the whole scene.
(2) Geomagic Studio. Wrap the tree points into a triangular mesh.
(3) 3ds Max. Draw spline lines manually

along the stems: skeleton of the tree.
(4) 3ds Max. Generate columns along the spline lines using the tool "loft".
(5) 3ds Max. Texture the loft as stems and the remaining triangles as canopy, using images captured in the field.

Figure 12 shows a tree modeled this way. Ten types of trees have been distinguished, but only three have been modeled at such detail so far.

A faster method consists in measuring in the UAV images with one point the top center of the canopy and the radius. This way we recorded about 2.000 trees. The height of the tree was obtained by projecting the top point onto the DTM. These measures can be used to fit a tree model.

Another object of interest are street light lamp poles. We measured and modeled about 900 of those lamp poles.

For each lamp pole we recorded in the MLS point cloud parameters such as type, location, size and direction by using Pointools ViewPro. Every lamp pole was meas-
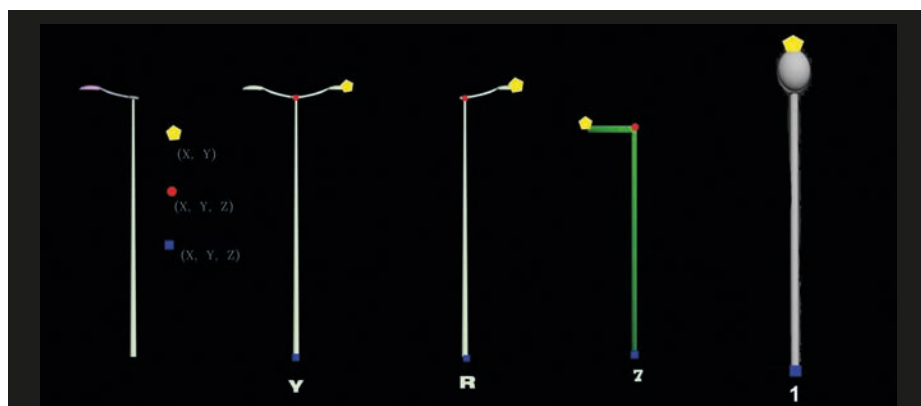
Figure 13: Types of lamp poles

ured by 2 to 3 points. With 3ds Max we built standard models for five types of lamp poles (Figure 13), which then were fit to the respective data.

6 CONCLUSIONS

This paper addresses a project of very high resolution 3D city modeling by integration of UAV images, terrestrial images and MMS point cloud data. This pilot project of creating a model of the NUS campus, Singapore delivers many valuable experiences for future applications and research

topics: (1) The accuracy of multiple data fusion is evaluated. (2) The experiment shows that using the UAV aerial image data to georeference MMS data is feasible and successful and can save a lot of surveying field work. (3) Complete building models are created by integration of UAV data, terrestrial images and MMS data.

However, the problems we met in this project also show the directions of our future work: (1) How to improve the level of automation in georeferencing of MMS data? (2) How to improve the accuracy of

data registration by utilizing features from both data sources? (3) How to do the micro-adjustment to achieve a perfect match between building roofs with the façade model? (4) How to improve and speed up the façade modeling procedure?

From our working experience in this project we also found that convenient tools for multi-sensor integrated modeling are still not available, which indicates a topic which needs more attention in future R&D.

The project is work in progress. We still have to process most of the terrestrial images and we also have flown UAV oblique images for a certain section of the area to have another useful information channel. This will enter an automated georeferencing and point cloud generation system to compare the results with manual and semi-automated approaches. So far most work has been done manually or semi-automatically using CyberCity Modeler. We also will use the data for change detection tasks. Another ongoing effort relates to the use of the data for building up an information system.

References

Al-Manasir, K.; Fraser, C. S. (2006): Automatic registration of terrestrial laser scanning data via imagery. In: Int. Arch. Photogramm. Remote Sens. Spatial Inf. Sci., XXXVI (Part 5), pp. 26-31.

Deseilligny, P. M.; Clery, I. (2011): APERO, an open source bundle adjustment software for automatic calibration and orientation of sets of images. In: Int. Arch. Photogramm. Remote Sens. Spatial Inf. Sci., XXXVIII-5/W16, pp. 269-276.

Eisenbeiss, H. (2009): UAV photogrammetry. Diss. ETH., No. 18515. doi:10.3929/ethz-a-005939264.

Gruen, A.; Wang, X. (1998): CC-Modeler: a topology generator for 3-D city models. In: ISPRS Journal of Photogrammetry and Remote Sensing, pp. 286-295.

Gruen, A.; Zhang, Z.; H. Eisenbeiss, H. (2012): UAV Photogrammetry in remote areas – 3D modeling of Drapham Dzong, Bhutan. Invited Paper ISPRS Congress, Melbourne. In: Int. Arch. Photogramm. Remote Sens. Spatial Inf. Sci., XXXIX-B1, pp. 375-379.

Irschara, A.; Kaufmann, V.; Klopschitz, M.; Bischof, H.; Leberl, F. (2010): Towards fully automatic photogrammetric reconstruction using digital images taken from UAVs. Proceedings International Society for Photogrammetry and Remote Sensing Symposium, 100 Years ISPRS – Advancing Remote Sensing Science.

Lowe, D. (2004): Distinctive image features from scale-invariant keypoints. In: International Journal of Computer Vision, 60 (2), pp. 91-110.

Maurer, M.; Rumpler, M.; Wendel, A.; Hoppe, C.; Irschara, A.; Bischof, H. (2012): Geo-referenced 3D reconstruction: Fusing public geographic data and aerial imagery. In: Proceedings of the International Conference on Robotics and Automation (ICRA), St. Paul, Minnesota (USA), 2012.

Remondino, F.; Fraser, C. S. (2006): Digital camera calibration methods: considerations and comparisons. In: Int. Arch. Photogramm., Remote Sens. Spatial Inf. Sci., XXXVI (Part 5), pp. 266-272.

Rutzinger, M.; Elberink, S. O.; Pu, S.; Vosselman, G. (2009): Automatic extraction of vertical walls from mobile and airborne laser scanning data. In: Int. Arch. Photogramm. Remote Sens. Spatial Inf. Sci., 38 (Part 3), W8.

Stewart, J. P.; Hu, J.; Kayen, R. E.; Lembo Jr., A. J.; Collins, B. D.; Davis, C. A.; O'Rourke, T. D. (2009): Use of airborne and terrestrial LIDAR to detect ground displacement hazards to water systems. In: Journal of Surveying Engineering, 135(3), pp. 113-124.

Von Hansen, W.; Gross, H.; Thoennessen, U. (2008): Line-based registration of terrestrial and airborne LIDAR data. In: Int. Arch. Photogramm. Remote Sens. Spat. Inf. Sci. 37, pp. 161-166.

Zuliani, M.; Kenney, M. C.; Manjunath, M. (2005): The multiransac algorithm and its application to detect planar homographies. IEEE International Conference on Image Processing, III-153-6.